http://dx.doi.org/10.5012/bkcs.2012.33.10.3473

CdSe Nanowire/Fullerene Nanocomposite Photoelectrode: Charge Separation and Photoelectrochemical Behavior

Ayoung Kim,[a] Jihee Lee,[a] Eun Joo Lee, and Jin Ho Bang[*]

Department of Chemistry and Applied Chemistry, Hanyang University, Ansan, Kyeonggi-do 426-791, Korea
[*]E-mail: jbang@hanyang.ac.kr
Received June 8, 2012, Accepted July 12, 2012

Key Words : CdSe nanowires, Fullerene, Nanocomposite, Electron transfer, Photoelectrochemistry

The fabrication of semiconductor nanocomposites with a staggered band-edge alignment has been widely adapted to facilitate charge separation, thus harnessing more photons in light-harvesting systems.[1] To date, a variety of semiconductor nanocomposites have been developed ranging from purely inorganic nanocomposites to organic/inorganic hybrid analogues.[2-7] Among the organic/inorganic hybrid nanocomposites, semiconductor/fullerene (C_{60}) based nanoheterostructures have been widely investigated due to the excellent electron-accepting ability of C_{60}.[8-14] While a wide variety of QD/C_{60} hybrid nanocomposites have been reported, no attempt has been made toward combining semiconductor nanowires (NWs) with C_{60} to date. In comparison to QDs, semiconductor NWs can be potentially advantageous in several respects when they serve as a light harvester because of their asymmetric geometry. Superior intrinsic properties induced by the one-dimensional nanostructure, such as higher charge carrier mobility and larger absorption cross section, are representative benefits they can provide.[15,16] In this study, we have for the first time examined the photoelectrochemical performance of photoelectrodes comprised of CdSe NWs and CdSe NWs/C_{60} nanocomposite and have investigated the beneficial effect of C_{60} as a coupling material. We found that the CdSe NWs/C_{60} photoelectrode showed considerably enhanced performance than its counterpart, CdSe NWs. To elucidate the improvement, electron transfer kinetics and optical properties of the nanocomposite were investigated in this work.

Figure 1(a) shows the UV-Vis absorption spectrum and TEM images of CdSe NWs grown *via* the solution-liquid-solid (SLS) growth process. The colloidal CdSe NWs exhibited typical absorption characteristics with a band edge absorption at ~700 nm. The broad absorption feature tailed down to ~712 nm, which corresponds to the bulk band gap of CdSe (1.74 eV). TEM analysis in Figure 1(b) and (c) revealed that the CdSe NWs were 1-2 μm long with widths of 12-18 nm. Our CdSe NWs were shorter and thicker than other typical colloidal NWs because the solvent employed in our study, octadecene, has much less coordination power than trioctylphosphine oxide (TOPO), which is the most frequently used solvent in NW syntheses.[17] Therefore, the growth rate in our synthesis was relatively high, which resulted in the production of short, thick NWs. The diameters of NWs were much larger than the bulk exciton Bohr radius of CdSe (5.6 nm), from which we speculate no quantum confinement effect is expected. This reasoning is supported by the absorption feature where no blue-shift is found. Selected-area electron diffraction (SAED) pattern inset in Figure 1(c) revealed that the obtained CdSe NWs were polycrystalline, which is in good accordance with XRD analysis (data not given).

Thin films of CdSe NWs and of CdSe NWs/C_{60} were prepared by electrophoretic deposition. In this study, the lifetime of photogenerated charge carriers in CdSe NWs was examined to obtain insight into charge recombination and charge injection processes. Figure 2 displays the fluorescence emission decay profile of CdSe NWs and CdSe NWs/C_{60} films. As observed in our previous reports, multi-exponential decay behavior was observed, which are attributed to both heterogeneity of samples and varying degree of surface defects.[13,18] Each decay trace was fitted with three exponential kinetics ($F(t) = a_1 \exp(-t/\tau_1) + a_2 \exp(-t/\tau_2) + a_3 \exp(-t/\tau_3)$), where a's are normalized weighting factors and τ's are lifetimes), and the average lifetimes, $\langle\tau\rangle$, of 1.29 and 0.45 ns were yielded for CdSe NWs and CdSe NWs/C_{60} using this equation: $\langle\tau\rangle = \Sigma(a_i\tau_i^2)/\Sigma(a_i\tau_i)$; see Table 1 for fitting parameters and fitting errors. The shorten lifetime found in the CdSe NWs/C_{60} nanocomposite implies that an additional deactivation pathway except charge recombination was created by coupling the NWs with C_{60}. Suppose that the observed faster emission decay in the CdSe NWs/C_{60} nanocomposite arises solely from electron transfer from CdSe to C_{60}, the apparent rate constants of electron injection could be estimated using the following equation: $k_{et} = 1/\langle\tau\rangle - 1/\langle\tau_0\rangle$, where $\langle\tau\rangle$ and $\langle\tau_0\rangle$ are the lifetime of CdSe NWs/C_{60} and of CdSe NWs, respectively. The apparent rate constant for the electron transfer process was calculated to be 1.4×10^9 s^{-1}, indicating the charge injection event occurs on ultrafast timescale.

Optical properties of both CdSe NWs and CdSe NWs/C_{60} films were investigated by diffuse reflectance UV-Vis spectroscopy. Figure 3(a) shows that the CdSe NWs film exhibited broad absorption, which matches well the optical response of CdSe NWs shown in Figure 1(a). Unlike the film

[a]These authors contributed equally to this work.

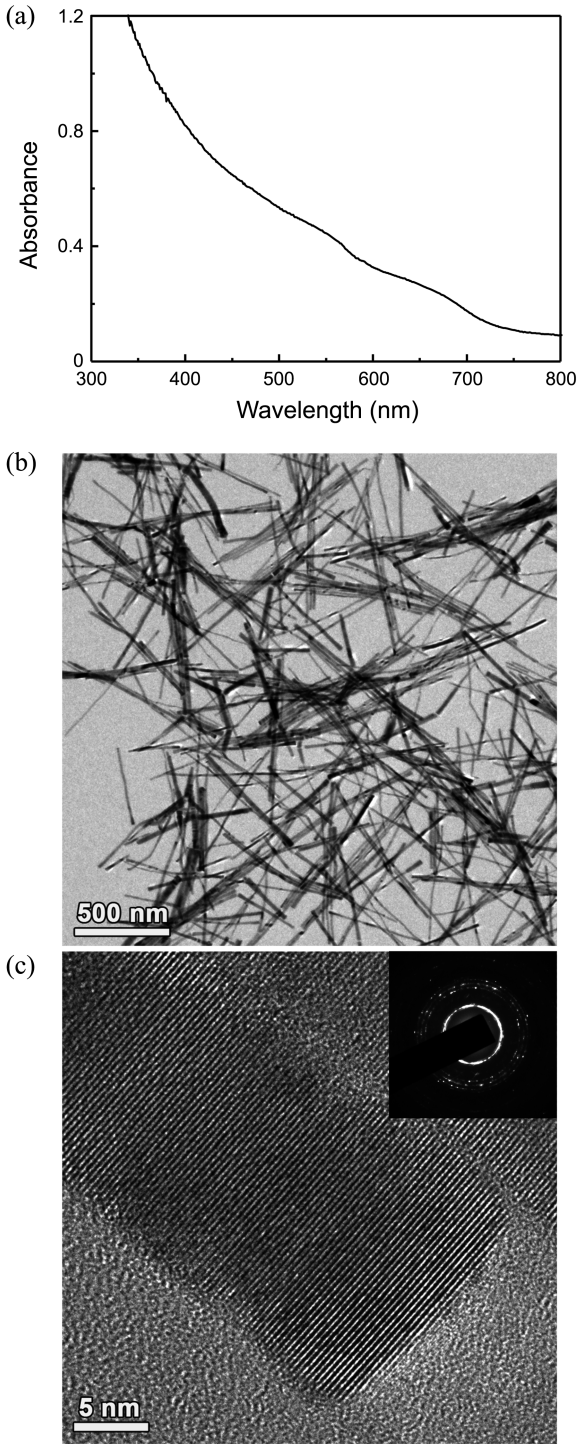

Figure 1. (a) UV-Vis absorption spectrum and (b and c) TEM images of CdSe NWs (inset: SAED of CdSe NWs).

prepared solely with CdSe NWs, additional broad absorption features were observed over the entire visible light region in

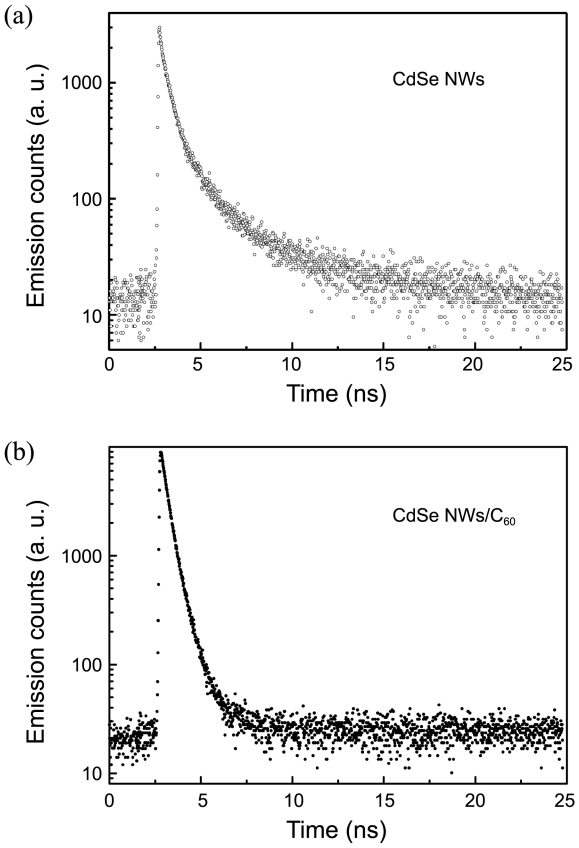

Figure 2. Emission decay profiles of (a) CdSe NWs and (b) CdSe NWs/C_{60}.

the case of the nanocomposite film, which is ascribed to the light scattering effect induced by C_{60} nanoclusters as noted in our previous report.[13] When deposited by electrophoretic deposition, C_{60} typically forms into clusters whose size ranges between 50 and 100 nm.[19] SEM micrographs in Figure 3(b) and (c) compare a different feature found in the morphology of CdSe NWs and CdSe NWs/C_{60} films. While the CdSe NWs film is a randomly packed NW assembly, the NWs are interwoven with the agglomerated C_{60} nanoclusters in the CdSe NWs/C_{60} film. Not only can the C_{60} nanoclusters serve as scattering centers which improve light absorption, but they are also capable of playing a role as an electron acceptor which retards charge recombination within CdSe NWs significantly, as proven in our emission decay study.

These films were evaluated as a photoelectrode in a three-electrode configuration.[20] Figure 4(a) compares the photoelectrochemical performance of the CdSe NWs and CdSe NWs/C_{60} films. Upon being illuminated, the CdSe NWs/C_{60} photoelectrode excelled in photocurrent generation in comparison to the CdSe NWs counterpart. Photocurrent generation by C_{60} photoelectrode was negligible, indicating that

Table 1. Emission Decay Analysis of CdSe NWs and CdSe NWs/C_{60}

	a_1	τ_1 (ns)	a_2	τ_2 (ns)	a_3	τ_3 (ns)	$\langle\tau\rangle$ (ns)	χ^2
CdSe NWs	0.07	0.09	0.58	0.54	0.35	2.80	1.29	1.18
CdSe NWs/C_{60}	0.03	0.05	0.71	0.35	0.26	0.78	0.45	1.19

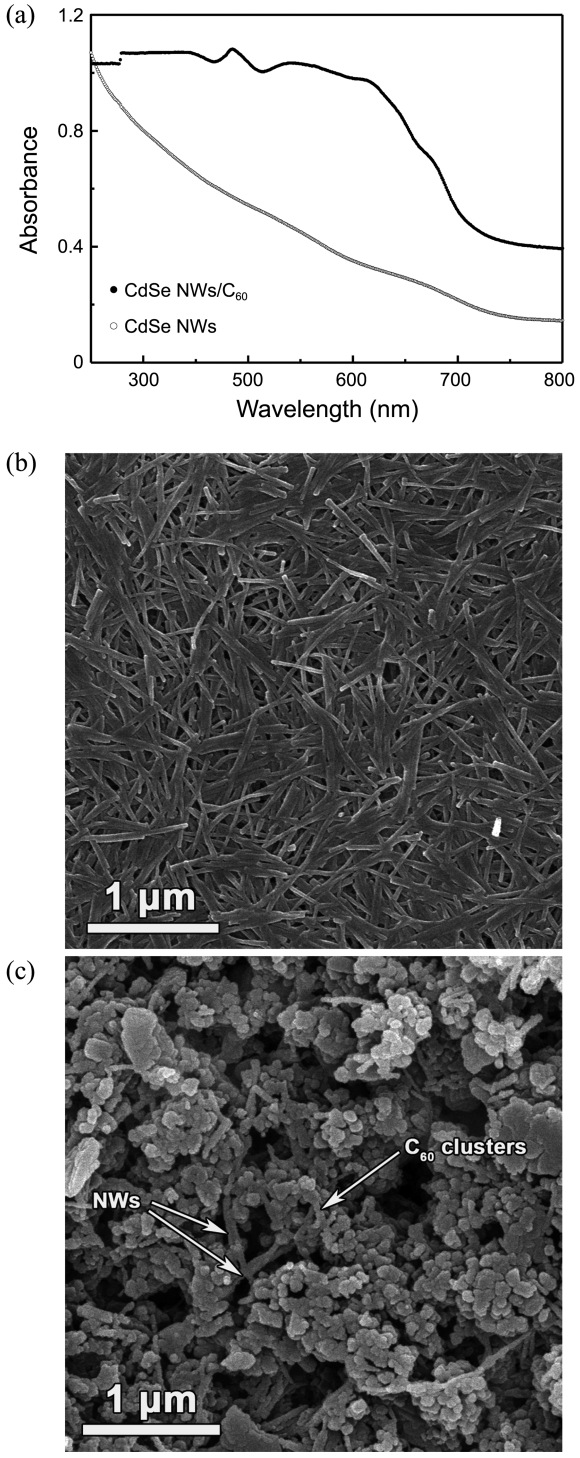

Figure 3. (a) Diffuse reflectance UV-Vis absorption spectra of CdSe NWs/C_{60} (solid dots) and CdSe NWs (open dots) and SEM images of (b) CdSe NWs and (c) CdSe NWs/C_{60} electrodes.

C_{60} solely serves as scattering center and electron acceptor. Manipulating the ratio of CdSe NWs and C_{60} would have an impact on photoelectrochemical performance (*e.g.*, we speculate that increasing the amount of CdSe NWs may bring further improvement), which is being investigated currently in our group. While the electrophoretic deposition was not fully optimized, this observation clearly proved the

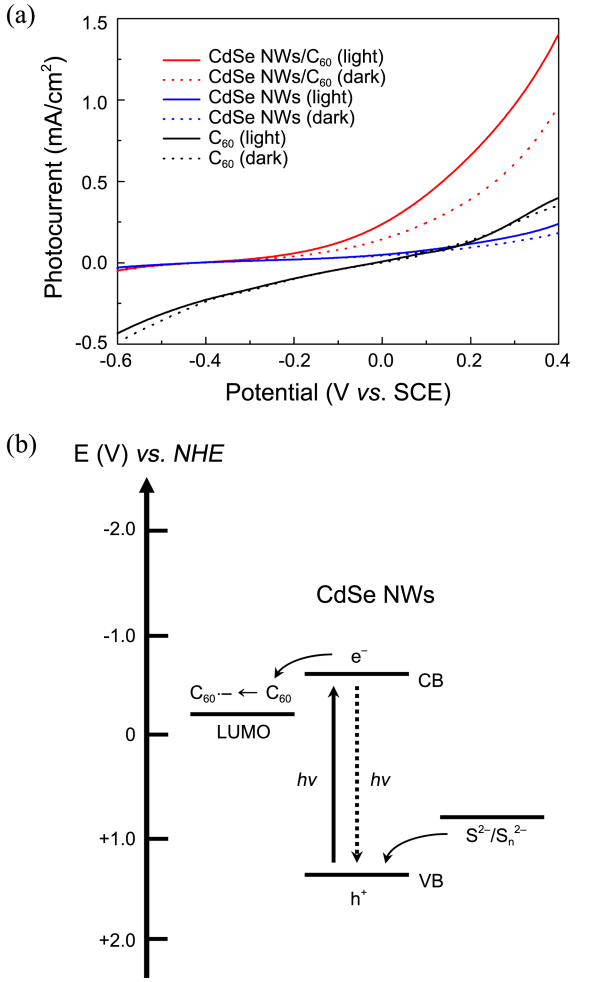

Figure 4. (a) Photoelectrochemical performance of CdSe NWs/C_{60} (red lines), CdSe NWs (blue lines), and C_{60} (black lines) electrodes ($\lambda > 300$ nm, 100 mW/cm^2) and (b) energy diagram of CdSe NWs/C_{60} electrode (LUMO: lowest unoccupied molecular orbital, CB: conduction band, VB: valence band, and NHE: normal hydrogen electrode).

effective photon harvesting in our CdSe NWs/C_{60} hybrid system. This result highlights the beneficial effect of C_{60}. As our optical study suggests, a significantly greater number of photons were absorbed by CdSe NWs when they were coupled with C_{60}. This implies that more photons can be converted to photocurrent. Along with the contribution from better light absorption, better charge separation occurred in the CdSe NWs/C_{60} photoelectrode accounts for the substantially enhanced performance. In our recent study with CdSe QDs, we have revealed that faster deactivation of charge-separated states occurs in CdSe QDs *via* the electron injection from CdSe QDs to C_{60}, which generates radical anion of C_{60} ($C_{60}^{\bullet-}$) as follows:[13]

$$\text{CdSe} + h\nu \longrightarrow \text{CdSe (h + e)} \longrightarrow \text{CdSe} + h\nu' \quad (1)$$

$$\text{CdSe/C}_{60} + h\nu \longrightarrow \text{CdSe (h)/C}_{60}^{\bullet-} \quad (2)$$

Given the band positions of CdSe NWs in energy diagram (close to those of bulk CdSe), it is reasonable to infer that the

same charge separation route can explain the charge separation process occurred in CdSe NWs. As depicted in Figure 4(b), therefore, photogenerated electrons are injected quickly into C_{60}, proven by our emission decay study, and they move along the C_{60} nanocluster network while CdSe NWs are regenerated by a redox couple. This continuous cycle boosts up photocurrent by suppressing charge recombination within CdSe NWs. Currently, we are optimizing our electrophoretic deposition process to further increase photoconversion efficiency.

In summary, colloidal CdSe NWs were coupled with C_{60} by electrophoretic deposition, and the electron transfer kinetics and photoelectrochemical performance of the resulting nanocomposite film were investigated. The photoelectrochemical performance of CdSe NWs/C_{60} hybrid electrode was superior to that of its counterpart, CdSe NWs electrode, which is attributed to significantly reduced charge recombination and improved light absorption induced by C_{60}. We believe this novel heterostructure provides a new way to develop an efficient photon harvesting system.

Experimental Section

Colloidal CdSe NWs were synthesized according to a previous report with some modification.[17] CdO (64.2 mg), oleic acid (0.40 mL), and octadecene (5 mL) were degassed at 80 °C under N_2 atmosphere. The temperature of the mixture was then raised to 300 °C. During the heating, the mixture turned into a colorless solution, indicating the formation of cadmium oleate. At 300 °C, an aliquot consisting of selenium (1 M) dissolved in trioctylphosphine (25 μL) and $BiCl_3$ (2 mM, 12.5 μL) in acetone was injected into the solution. Upon the injection, the color of the solution turned black immediately, and the temperature was held at 260 °C for 3 min. After the reaction, the solution was cooled to room temperature, washed with a mixture of methanol and toluene (v/v = 3:7) to remove unwanted QDs, and dissolved in toluene for use.

For the characterization of the CdSe NWs, an ultraviolet-visible (UV-Vis) spectrophotometer (SCINCO S-3100), an X-ray diffractometer (Rigaku D/Max-2500/PC), and a transmission electron microscope (JEOL 2010F) were employed. In order to prepare photoelectrodes, a solution of CdSe NWs and a blend of CdSe NWs (optical density at 670 nm: 2, 0.5 mL) and C_{60} (1 mM, 0.5 mL) in toluene/acetonitrile solvent (v/v = 1:4) were electrophoretically deposited onto SnO_2-coated OTE as previously described in our report.[13] The morphology of each photoelectrode was examined using a field-emission scanning electron microscope (Hitachi S-4800 FESEM), and the absorption characteristics were examined using a Perkin Elmer spectrophotometer (Lambda 750). Fluorescence emission lifetime measurement of both photoelectrodes was carried out using an inverse time-resolved fluorescence microscope (PicoQuant, MicroTime-200) with 470 nm laser excitation. Current-voltage characteristics of the photoelectrodes were recorded using a potentiostat (CH Instruments, CHI 660D) at a scan rate of 50 mV/s in a three-electrode configuration using Pt gauze as a counter electrode and a saturated calomel electrode (SCE) as a reference electrode. An aqueous Na_2S solution (0.1 M) was employed for electrolyte, and N_2 gas was purged through the electrolyte for 15 min to ensure oxygen-free atmosphere. A 300 W xenon arc lamp equipped with air mass 1.5 filter (Oriel) served for a light source.

Acknowledgments. This work was supported by the research fund of Hanyang University (HY-2010-N).

References

1. Kamat, P. V.; Tvrdy, K.; Baker, D. R.; Radich, J. G. *Chem. Rev.* **2010**, *110*, 6664.
2. Nozik, A. J.; Beard, M. C.; Luther, J. M.; Law, M.; Ellingson, R. J.; Johnson, J. C. *Chem. Rev.* **2010**, *110*, 6873.
3. Vogel, R.; Hoyer, P.; Weller, H. *J. Phys. Chem.* **1994**, *98*, 3183.
4. Hodes, G. *J. Phys. Chem. C* **2008**, *112*, 17778.
5. Bang, J. H.; Kamat, P. V. *Adv. Funct. Mater.* **2010**, *20*, 1970.
6. Buhbut, S.; Itzhakov, S.; Oron, D.; Zaban, A. *J. Phys. Chem. Lett.* **2011**, *2*, 1917.
7. Nayak, P. K.; Bisquert, J.; Cahen, D. *Adv. Mater.* **2011**, *23*, 2870.
8. Liu, D.; Wu, W.; Qiu, Y.; Lu, J.; Yang, S. *J. Phys. Chem. C* **2007**, *111*, 17713.
9. Brown, P.; Kamat, P. V. *J. Am. Chem. Soc.* **2008**, *130*, 8890.
10. Song, N.; Zhu, H.; Jin, S.; Zhan, W.; Lian, T. *ACS Nano* **2010**, *5*, 613.
11. Guldi, D. M.; Zilbermann, I.; Anderson, G.; Kotov, N. A.; Tagmatarchis, N.; Prato, M. *J. Am. Chem. Soc.* **2004**, *126*, 14340.
12. Li, Y.; Mastria, R.; Fiore, A.; Nobile, C.; Yin, L.; Biasiucci, M.; Cheng, G.; Cucolo, A. M.; Cingolani, R.; Manna, L. *et al. Adv. Mater.* **2009**, *21*, 4461.
13. Bang, J. H.; Kamat, P. V. *ACS Nano* **2011**, *5*, 9421.
14. Narayanan, R.; Reddy, B. N.; Deepa, M. *J. Phys. Chem. C* **2012**, *116*, 7189.
15. Giblin, J.; Kuno, M. *J. Phys. Chem. Lett.* **2010**, *1*, 3340.
16. Schafer, S.; Wang, Z.; Zierold, R.; Kipp, T.; Mews, A. *Nano Lett.* **2011**, *11*, 2672.
17. Puthussery, J.; Kosel, T. H.; Kuno, M. *Small* **2009**, *5*, 1112.
18. Bang, J. H.; Kamat, P. V. *ACS Nano* **2009**, *3*, 1467.
19. Kamat, P. V.; Barazzouk, S.; Thomas, G.; Hotchandani, S. *J. Phys. Chem. B* **2000**, *104*, 4014.
20. Hodes, G. *J. Phys. Chem. Lett.* **2012**, *3*, 1208.